



Identification of performance limiting electrode using asymmetric cell configuration in vanadium redox flow batteries

Ertan Agar, C.R. Dennison, K.W. Knehr, E.C. Kumbur*

Electrochemical Energy Systems Laboratory, Department of Mechanical Engineering and Mechanics, Drexel University, Philadelphia, PA 19104, USA

HIGHLIGHTS

- Performance of a VRFB is investigated using asymmetric electrode configuration.
- Three different electrodes (i.e., raw, acid- and heat-treated) are investigated.
- Electrode functionalization is found to have different effects on (+) and (–) half-cells.
- Negative half-cell reactions are found to limit the overall performance of a VRFB.
- Poor performance of (–) half-cell is due to the undesired hydrogen evolution.

ARTICLE INFO

Article history:

Received 25 August 2012

Received in revised form

4 October 2012

Accepted 8 October 2012

Available online 16 October 2012

Keywords:

Carbon felt

Cyclic voltammetry

Electrode

Reaction kinetics

Vanadium flow battery

ABSTRACT

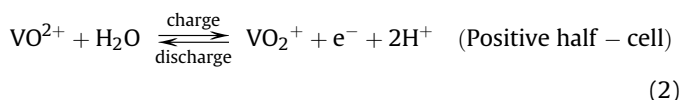
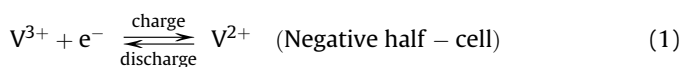
In this study, the performance of a vanadium redox flow battery (VRFB) is investigated using asymmetric electrode configurations with raw and functionalized (i.e., acid-treated and heat-treated) electrodes. The use of heat-treated electrodes in both half-cells is chosen as the baseline case for comparison, as this configuration shows the best performance. When the positive electrode in the baseline case is replaced with a raw or acid-treated electrode, the voltage efficiency is found to be comparable to that of the baseline case. However, in the case where the negative electrode in the baseline case is replaced with a raw or acid-treated electrode, a significantly lower efficiency is observed, suggesting that the negative half-cell reactions limit the performance of a VRFB. To further investigate this observation, an additional analysis is performed using cyclic voltammetry. The reaction kinetics data suggests that the poor performance of the negative half-cell is not due to the slow kinetics, but rather stems from the fact that the reduction reaction in the negative half-cell occurs at a potential that is very close to the onset of hydrogen evolution. The formation of hydrogen gas bubbles blocks the reaction sites and suppresses the favorable effects of functionalization in the negative half-cell.

© 2012 Elsevier B.V. All rights reserved.

1. Introduction

The vanadium redox flow battery (VRFB) is an emerging energy storage technology, which offers unique advantages for use in large-scale energy storage. Unlike conventional batteries, the electrolytes are stored in external tanks and are circulated through an electrochemical cell. The key advantage of these systems is that power generation and energy storage are decoupled such that the energy storage capacity is determined by the amount of electrolyte in the storage tank and the electrolyte composition, whereas the power rating depends on the active surface area available for the electrochemical reactions in the VRFB cell [1,2].

A VRFB cell is composed of two inert porous electrodes which provide sites for the reactions, and an ion exchange membrane, which allows for ion transport between the half-cells to maintain electro-neutrality. The electrolytes in half cells are composed of differently oxidized vanadium species dissolved in sulfuric acid. The energy conversion process in half-cells occurs via following redox reactions:



where VO^{2+} and VO_2^+ represent vanadium in the V(IV) and V(V) oxidation states, respectively.

* Corresponding author. Tel.: +1 215 895 5871; fax: +1 215 895 1478.

E-mail address: eck32@drexel.edu (E.C. Kumbur).

A key component that dictates the VRFB performance is the porous electrode which is responsible for enabling electrolyte transport, facilitating ion/charge transfer and providing reaction sites for electrochemical reactions. The internal structure and surface chemistry of the electrodes have direct implications on the transport related losses, electrolyte utilization, charge resistance and performance degradation. For instance, the available surface area in the electrode has a profound effect on the electrolyte utilization and system power output. In a recent study, Mench and his coworkers [3] have shown that the system performance can be significantly enhanced by increasing the total surface area of the electrodes. Similarly, the surface chemistry of the electrode governs the activation energy required to initiate the half-cell reactions. Depending upon the nature of the reactions, the surface chemistry of the electrodes may have an adverse effect on the reaction kinetics, which typically manifests itself as a decrease in output voltage and system efficiency.

Due to the highly oxidizing nature of V(V) ions, carbon and graphite are among the few materials that can be employed as electrodes in VRFBs [4,5]. In order to find the most compatible option, a variety of carbon based electrode materials (e.g., carbon nanotubes, oxidized graphite felt, and carbon-polymers) have been explored [6–9]. Among these, graphite felts, carbon cloths, and carbon fibers are shown to be the most promising candidates as they offer relatively high specific surface areas at a reasonable cost [10]. However, one major problem with these electrodes is that they possess very poor electrochemical activity, therefore showing poor kinetics for half-cell vanadium reactions. To address this issue, significant effort has been placed on improving the surface chemistry of these materials by introducing various functional groups [4,11–15]. Sun and Skyllas-Kazacos [11,12] have investigated the effects of thermal and acid treatments on the surface chemistry of carbon felt electrodes. Their studies indicate that surface treatment significantly increases the surface functional groups C–O and C=O at the electrode surface, which enhances the reaction rate in each half-cell. Similarly, Zhong et al. [13] and Yue et al. [4] have shown that introducing –OH and C=O groups considerably increases the electrochemical activity, reducing the activation overpotential of the electrodes. More recently, Wang and Wang [14] performed a study on Ir³⁺ catalyzed electrodes. The Ir-modified electrode yielded very good electrochemical activity, particularly for the V(IV)/V(V) reaction. However, results for V(II)/V(III) reaction showed very poor activity, indicating that the use of same functionalization methods for both electrodes may not provide the desired performance.

Although the advantages of heat or acid treatment of the electrodes on the overall VRFB performance are repeatedly expressed in the literature, the exact contribution of these surface treatment methods on the positive and negative half-cell reactions remains unknown. Due to the different nature of the reduction and oxidation reactions, one of these redox reactions may limit the overall performance of the system. As a result, the same functionalization method might not be beneficial or appropriate for both half-cell electrodes. One potential approach to address this issue would be to identify the limiting half-cell reaction through a detailed analysis of the reaction kinetics in each half-cell. To date, studies reported in literature have been performed using symmetric configurations, where the same type of electrode (i.e., treated via the same functionalization method) was used for both positive and negative half-cells. As a result, it is very challenging to extract the key information from these studies with regards to which half-cell reaction is limiting the overall system performance. Such information would be very useful to understand the role of side reactions (e.g., hydrogen or oxygen evolution) on surface treatment and help to determine the optimum functionalization protocol for the VRFB electrodes.

In addition to the surface functionalization, understanding the reaction kinetics in each half-cell would have a direct impact on improving the resolutions of the VRFB models. Due to the paucity of experimental data, to date, the majority of the input parameters used in VRFB models are approximated or used as fitting parameters [16–24]. For instance, in the literature, very little information is available regarding reaction kinetic parameters, such as reaction rate constant (k) and charge transfer coefficient (α), for the carbon felt electrodes. As a result, nearly every VRFB model uses the same reaction rate constant for both oxidation and reduction reactions. Moreover, most models assume that the charge transfer coefficient, α , is equal to 0.5, though this has not been validated. Since the oxidation and reduction reactions in each half cell occur at different rates, it is very likely that the use of same reaction rate constants for both half-cell reactions might potentially yield inaccurate predictions of the activation overpotential and the cell potential.

This study is motivated by the need to better understand the half-cell reactions and their effects on the electrode functionalization. Our specific objective was to determine the limiting half-cell reaction by conducting performance analysis on differently functionalized VRFB electrodes using *asymmetric* electrode configurations (i.e., using different electrodes in positive and negative half-cells). Three different carbon felt electrode types, namely: raw, acid-treated and heat-treated electrodes were investigated via charge/discharge cycle testing. Cyclic voltammetry measurements were also conducted to determine the role of side reactions on the surface functionalization and quantify the key kinetic parameters, such as reaction rate constant and the charge transfer coefficient, for each electrode type, to provide a reliable set of input parameters for modeling efforts.

2. Method of approach

2.1. Electrochemical flow cell and electrolyte preparation

Charge/discharge cycling tests were conducted using a 10 cm² flow cell equipped with two composite graphite current collectors and two GFA5 (SGL Carbon Group, Germany) carbon felt electrodes, separated by a Nafion® 117 membrane. The GFA5 electrodes are made of a loose, random weave of graphitized carbon fibers with a thickness ranging from 2 to 5 μ m (see Fig. 1). Both raw and treated (i.e., heat-treated and acid-treated) GFA5 electrodes, which have 5 mm nominal thickness and 20% compression when the flow cell is assembled, were tested in this study. Heat treatment was performed by oxidizing the raw electrode at 400 °C in an air atmosphere for 6 h [13], while the acid treatment was performed by boiling the electrodes in 98% sulfuric acid for 6 h. Prior to testing, the Nafion® membrane was submerged in H₂O₂ for 60 min at 80 °C, and then was placed in boiling deionized water for 60 min. After this step, the membrane was put into 0.5 M H₂SO₄ at 80 °C for 60 min, and then rinsed in boiling water for 60 min to remove any excess acid [25].

The electrolytes were prepared by filling each half-cell reservoir with a 60 ml solution of 1 M VOSO₄ (Sigma Aldrich, 97% purity) in 4 M H₂SO₄. Both reservoirs were de-aerated by bubbling nitrogen through the solution for 1 h. The electrolyte solutions were charged potentiostatically at 1.7 V to produce V³⁺ and VO₂⁺ for the negative and the positive half-cell reactions, respectively [26]. The positive half-cell solution was then replaced with 60 ml of the initial 1 M VOSO₄ solution to achieve an electrolyte solution that consists of 1 M V³⁺ in 3.5 M H₂SO₄ in the negative half-cell and 1 M VO₂⁺ in 4 M H₂SO₄ in the positive half-cell [27]. During charge/discharge testing, the electrolytes were stored under a continuous nitrogen blanket to prevent oxidation of the active species.

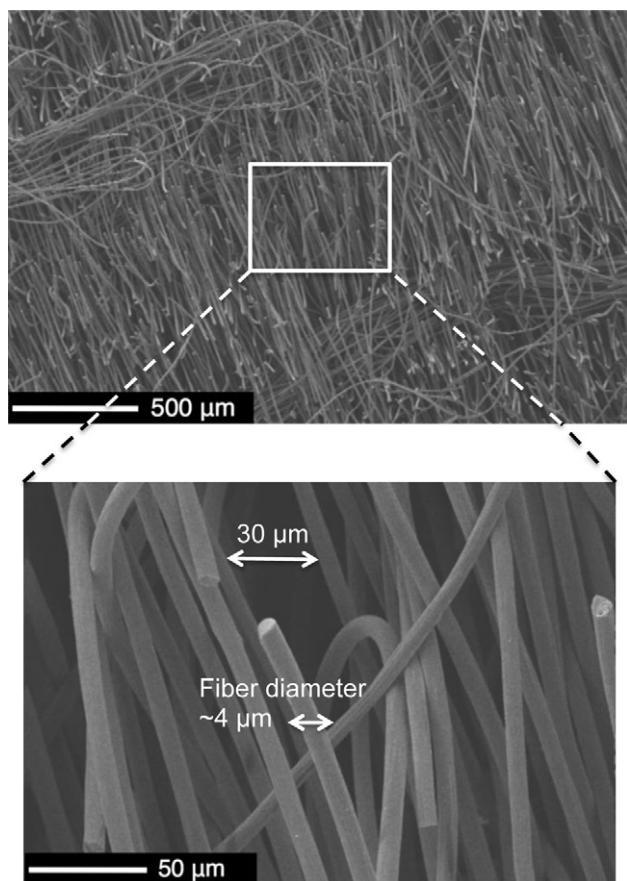


Fig. 1. SEM image of raw (as delivered) GFA5 carbon felt electrode used in this study.

2.2. Charge/discharge cycling

The charge/discharge cycling of the VRFB cell was performed using an in-house flow battery testing station. In order to minimize experimental cycling time, the system was operated in a static (no flow) configuration. The cell was charged to a maximum potential of 1.7 V and then discharged to a minimum potential of 0.8 V at a constant current density of 40 mA cm⁻². During galvanostatic charging and discharging, open circuit voltage was recorded for each step. Two sets of experiments with symmetric and asymmetric electrode configurations were performed.

For the symmetric configuration, the same type of electrodes (e.g., raw/raw, acid-treated/acid-treated, and heat-treated/heat-treated) were used in both half cells, and the performance of the system was measured using charge/discharge testing. For testing with the asymmetric electrode configuration, two different case studies (i.e., Case 1 and Case 2) were performed. In Case 1, a heat-treated electrode was used in the *negative* half-cell, while each of the three types of electrodes (i.e., raw, acid-treated, and heat-treated) was used separately in the positive half-cell. In Case 2, a heat-treated electrode was used in the *positive* half-cell, while the tested electrode types were interchanged in the negative half-cell. A schematic describing these two case studies is shown in Fig. 2.

2.3. Cyclic voltammetry

A three-electrode electrochemical cell composed of an Ag/AgCl reference electrode, platinum wire counter electrode, and a carbon felt working electrode, was used for cyclic voltammetry analysis. A Luggin capillary was used to provide a precise sensing point for the

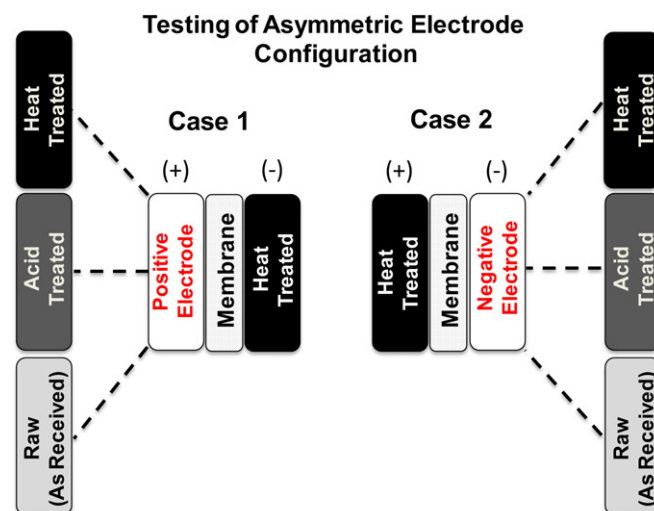


Fig. 2. Schematic of the asymmetric cell configuration testing. Case 1: Heat-treated electrode is used at the negative half-cell, while positive electrode is varied. Case 2: Heat-treated electrode is used at the positive half-cell, while negative electrode is varied.

reference electrode. In these experiments, cyclic voltammograms were obtained at 0.3 M VOSO₄ and 2 M H₂SO₄ concentration for the positive half-cell reaction and at 0.05 M VOSO₄ and 1 M H₂SO₄ concentration for the negative half-cell reactions. Cyclic voltammetry data were collected at 1, 2, 3, 4, and 5 mV s⁻¹ scan rates for each electrodes (i.e., raw, acid-treated and heat-treated). For the positive half-cell reactions, a voltage window of 0.4–1.4 V vs. Ag/AgCl was used, and this voltage window was varied slightly for each case in order to minimize the oxygen evolution and maintain the reduction of VO²⁺. Similarly, for the negative half-cell, a voltage window of –0.7–0.1 V vs. Ag/AgCl was used to reduce the hydrogen evolution and maintain the oxidation of V³⁺.

3. Results and discussion

3.1. Charge/discharge analysis using symmetric and asymmetric configurations

The results of the charge/discharge cycling tests in the symmetric electrode configuration (i.e., same electrode in each half-cell) are shown in Fig. 3. The tests were conducted at a constant current density of 40 mA cm⁻². As shown in Fig. 3, significant variation in the system performance was observed for the tested electrodes, especially for the heat-treated electrode. Voltage efficiencies of 62.4%, 68.8%, and 87.1% were found for the raw, acid-treated and heat-treated electrodes, respectively (see Table 1). Since each of these three electrodes is made of the same carbon felt, it is reasonable to assume that the electrodes have the same porosity, surface area, and resistivity. Therefore, the significant variation in measured voltage efficiency and performance can be attributed to the differences in electrode treatment methods. The results in Fig. 3 show that heat and acid treatment of the electrodes (especially the heat-treated electrode) increase the performance of the overall system, which agrees with the findings reported in literature [8,10–14].

In order to distinguish the effects of the treatment methods on the individual half-cell reactions (V²⁺/V³⁺ and VO²⁺/VO₂⁺), the charge/discharge cycling test was also conducted by using an asymmetric electrode configuration. For the first case study (Case 1, see Fig. 2), the heat-treated carbon felt was used at the negative

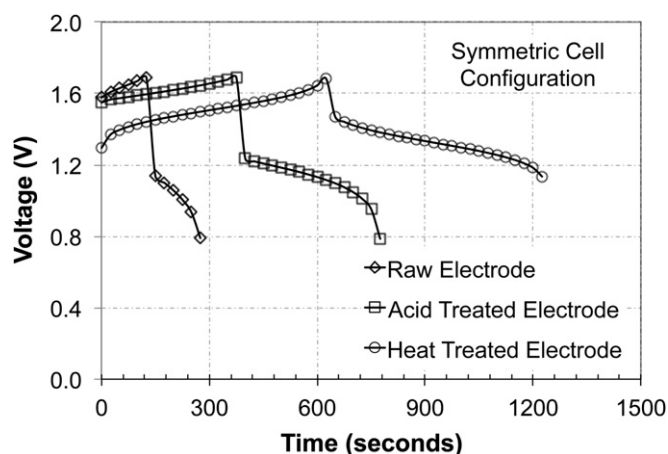


Fig. 3. Charge/discharge analysis of VRFB cell using a symmetric electrode configuration (i.e., same electrode used in both half-cells).

half-cell while each of the three different electrodes (i.e., raw, acid-treated and heat-treated) was interchanged in the positive half-cell. The heat-treated electrode was selected as the control case in the negative half-cell as it shows the best performance in the symmetric configuration, thus minimizing any performance limitations imposed by the control electrode. For each case, the galvanostatic charge/discharge cycling test was performed at 40 mA cm^{-2} , and the measured performance curves are shown in Fig. 4a. Fig. 4a indicates that the charge/discharge performance of the tested configurations in Case 1 has very similar behavior, although there are some small deviations. The voltage efficiencies for Case 1 are found to be 85.1%, 85.0%, and 87.1% for the raw, acid-treated, and heat-treated electrodes, respectively (Table 1). The small differences in measured voltage efficiencies indicate that the surface functionalization appears to have *minimal* impact on the reaction kinetics at the *positive* half-cell.

For the second case study (Case 2), the heat-treated electrode was used in the positive half-cell while all three electrode types were interchanged in the negative half-cell. As in Case 1, a galvanostatic charge/discharge cycle test was conducted at 40 mA cm^{-2} for all three configurations. Fig. 4b shows that the performance of the whole-cell changes significantly for the tested configurations in Case 2. Accordingly, a large variation in voltage efficiency (i.e., 60.3% for the raw electrode, 71.9% for the acid-treated and 87.1% for the heat-treated electrode) was observed within these three tested configurations. The significant variation in system performance and voltage efficiency indicate that the surface functionalization (which is observed to have minimal impact on the reaction at the positive half-cell in Fig. 4a), has a substantial effect on the kinetics of the *negative* half-cell reaction. In other words, the negative reaction appears to significantly benefit from the existence of additional functional groups that were introduced on the surface of the carbon felt electrodes. In addition, the comparison of the performance of

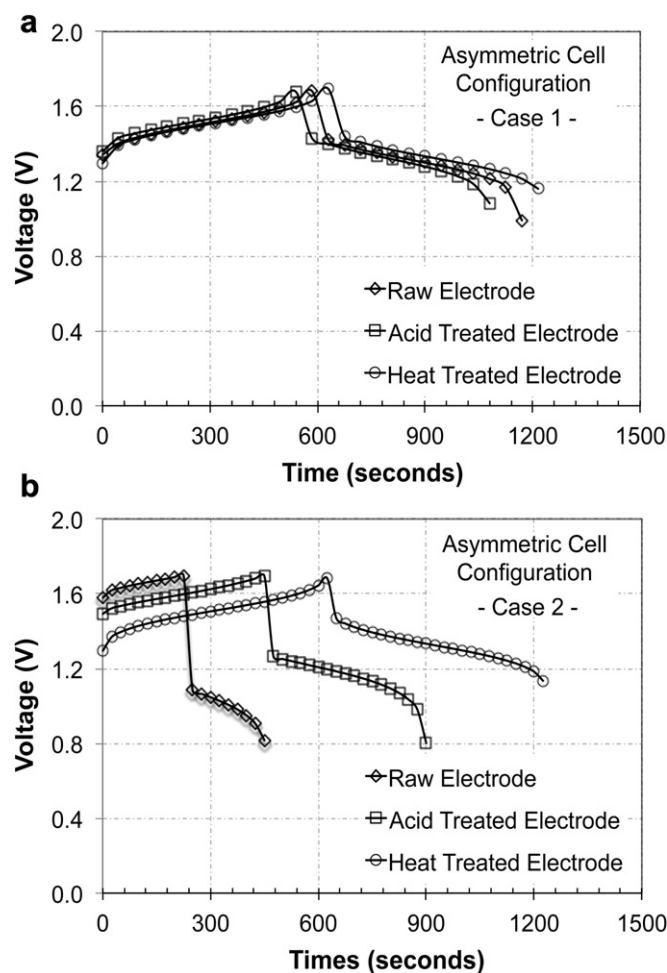


Fig. 4. Performance analysis of the VRFB using an asymmetric electrode configuration: (a) Case 1: Heat-treated electrode in the negative half-cell while positive electrode is varied by raw, acid-treated, and heat-treated electrodes; (b) Case 2: Heat-treated electrode in the positive half-cell while negative electrode is varied by raw, acid-treated, and heat-treated electrodes.

the raw electrode configuration between Case 1 and Case 2 (Fig. 4a and b) indicates that the negative half-cell reaction has significantly higher activation overpotential than the positive half-cell reaction. These observations suggest that the reaction kinetics at the negative half-cell appears to limit the voltage efficiency and power output of the VRFB, therefore for enhanced performance, special attention needs to be given to the surface treatment method used for functionalization of the negative half-cell electrode.

3.2. Reaction rate constants and charge transfer coefficients

The cyclic voltammetry analysis was performed for both half-cell redox reactions on all three electrode samples to compare the electrochemical behavior of the tested electrodes and quantify the standard rate constants (i.e., reaction rate constant, k , and charge transfer coefficient, α) of the oxidation and reduction reactions in the positive and negative half-cells. The cyclic voltammograms were obtained at $1\text{--}5 \text{ mV s}^{-1}$ scan rates and the standard rate constants were determined using the following relationship [28]:

$$i_p = 0.227nFAC_0ke^{-\frac{\alpha nF}{RT}(E_p - E^0)} \quad (3)$$

where i_p is the peak current, n is the number of electrons involved in the reaction, F is Faraday's constant, A is the active surface area of

Table 1

Measured voltage efficiencies using symmetric and asymmetric cell configurations. For the asymmetric cell configuration, the heat-treated electrode is used as the negative electrode in Case 1, whereas the heat-treated electrode is used as the positive electrode in Case 2.

Electrode	Symmetric configuration	Asymmetric configuration	
		Case 1	Case 2
Raw	62.36%	85.13%	60.34%
Acid-treated	68.79%	85.00%	71.88%
Heat-treated	87.10%	87.10%	87.10%

the electrode, C_0 is the bulk concentration of oxidant, E_p is the peak potential, and E^0 is the formal potential. The correlation given in Eqn. (3) relates the measured peak current and the voltage separation (Figs. 5 and 6) to the kinetic performance of the electrode, which allows for quantification of the reaction rate constants and charge transfer coefficient using these measured values. For brevity, the information regarding how to obtain this correlation is not included in this paper, but a detailed description of this formulation can be found in Ref. [28].

Tables 2 and 3 summarize the measured reaction rate constants and the charge transfer coefficients of tested electrodes for both

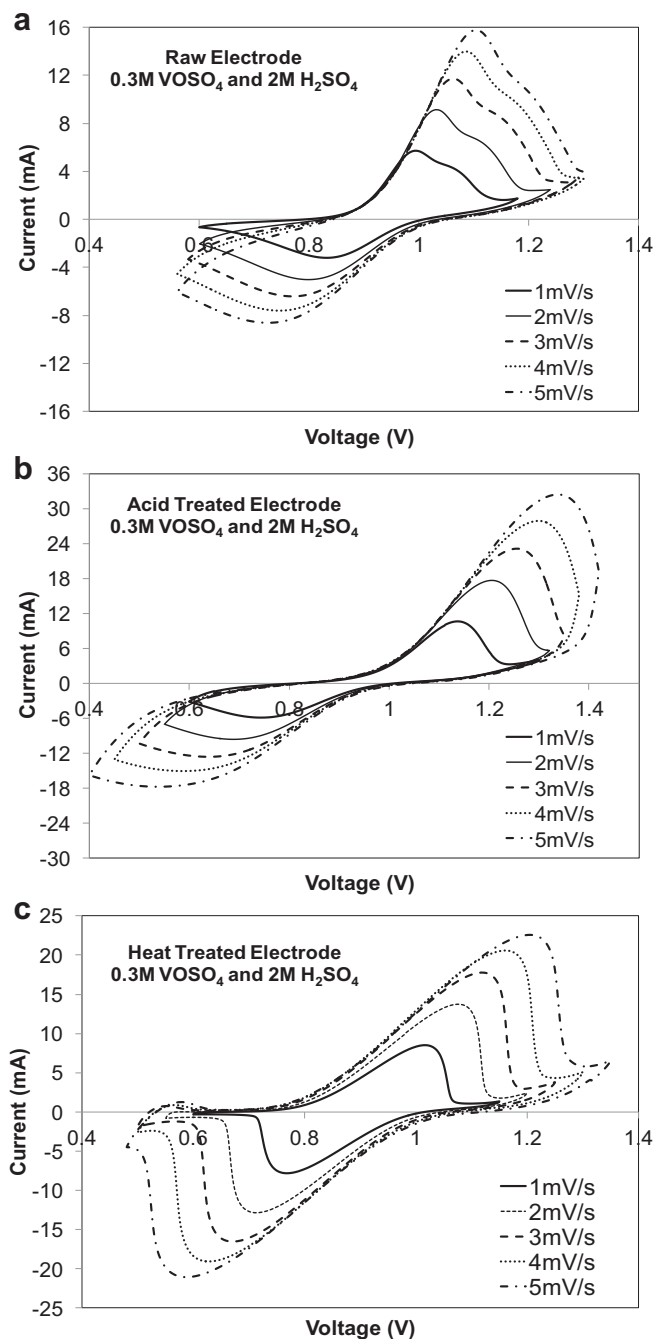


Fig. 5. Positive half-cell reactions: Cyclic voltammograms of 0.3 M VOSO_4 and 2.0 M H_2SO_4 on (a) raw, (b) acid-treated, and (c) heat-treated electrodes at 1, 2, 3, 4, and 5 mV s^{-1} .

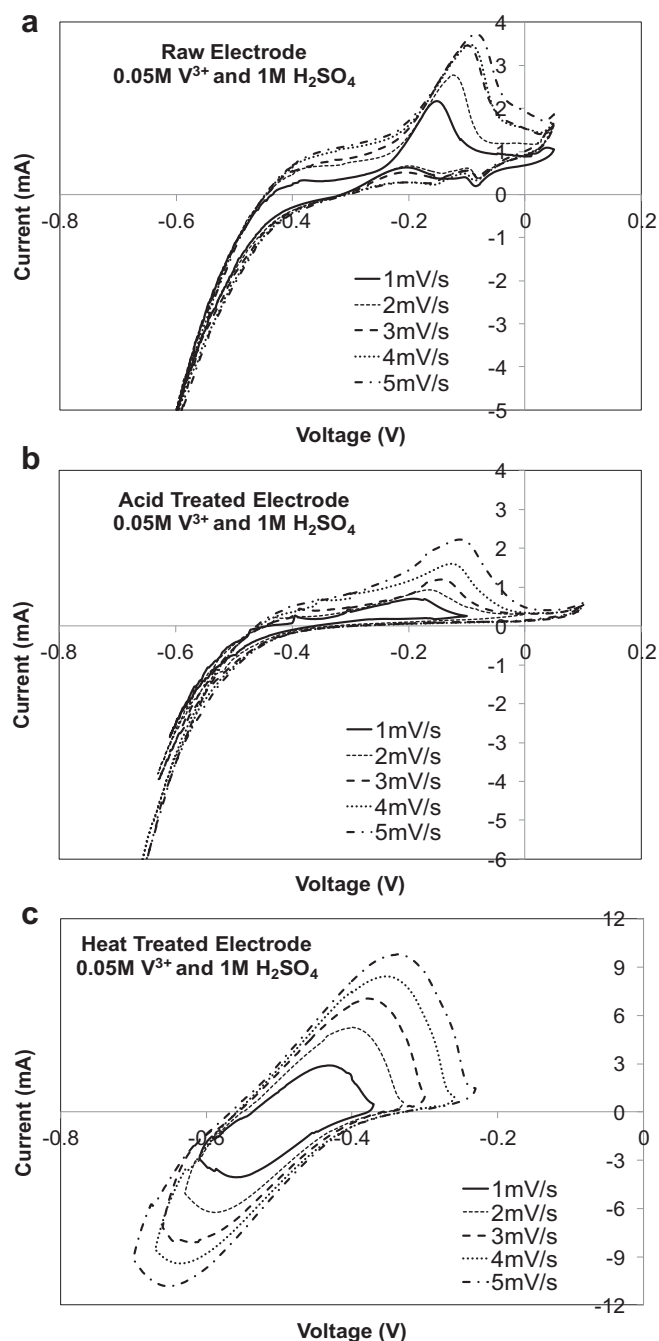


Fig. 6. Negative half-cell reactions: Cyclic voltammograms of 0.05 M V^{3+} and 1.0 M H_2SO_4 on (a) raw, (b) acid-treated, and (c) heat-treated electrodes at 1, 2, 3, 4, and 5 mV s^{-1} .

positive and negative half-cell reactions. The calculated α values indicate that the redox reactions in both half-cells are highly asymmetric; therefore the use of same charge transfer coefficient values (i.e., $\alpha = 0.5$) in mathematical models may not be accurate to describe the reaction kinetics in half-cells. In terms of reaction rate constants, for the positive half-cell (Table 2), the oxidation reaction was found to be more favorable than the reduction reaction (i.e., higher k value) for all the tested electrodes. For both reactions, functionalized electrodes were found to have significantly higher reaction rates than the raw electrode. Among the electrodes, the heat-treated electrode was observed to have the highest reaction

Table 2

Calculated reaction rate constants and charge transfer coefficients of $\text{VO}^{2+}/\text{VO}_2^+$ reaction (positive electrode) for raw, acid-treated, and heat-treated carbon felt electrodes.

Electrode	Oxidation		Reduction	
	$k \text{ (m s}^{-1}\text{)}$	α	$k \text{ (m s}^{-1}\text{)}$	α
Raw	1.83×10^{-7}	0.2301	9.96×10^{-8}	0.2320
Acid-treated	2.45×10^{-7}	0.1384	1.47×10^{-7}	0.1310
Heat-treated	3.12×10^{-7}	0.1310	2.79×10^{-7}	0.1352

Table 3

Calculated reaction rate constants and charge transfer coefficients of $\text{V}^{3+}/\text{V}^{2+}$ reaction (negative electrode) for raw, acid-treated, and heat-treated carbon felt electrodes.

Electrode	Oxidation		Reduction	
	$k \text{ (m s}^{-1}\text{)}$	α	$k \text{ (m s}^{-1}\text{)}$	α
Raw	1.54×10^{-7}	0.2071	NA	NA
Acid-treated	4.60×10^{-7}	0.3542	NA	NA
Heat-treated	5.47×10^{-7}	0.3144	8.38×10^{-7}	0.2588

rate for both half-cell reactions, which agrees with the results of the performance test shown in Fig. 3 (i.e., heat-treated electrode yielded higher voltage efficiency and average power output).

For the negative half-cell analysis, only the heat-treated electrode parameters could be determined since the reduction peaks were not observed for both raw and acid-treated electrodes (see Fig. 6). This is largely due to the fact that the onset of hydrogen evolution (i.e., the abrupt, linear decrease in the peak current at low voltages) occurred before a distinct reduction peak was observed for the raw and the acid-treated electrodes. When compared with the heat-treated electrode, the poor performance of the raw and the acid-treated electrodes can be attributed to the hydrogen evolution. The formation of hydrogen gas bubbles during charging blocks the reaction sites and reduces the active surface area, which impedes the reaction at the fiber surface and increases the activation losses. Therefore, one approach to minimize the activation losses in VRFBs would be to avoid using electrode materials in the negative half-cell which have incompatible surface chemistry and result in undesired hydrogen evolution. Significant increases in power density are likely possible by choosing electrode materials which are more kinetically selective to the V^{3+} reduction reaction and yield a peak potential for the reduction reaction which is outside the range of hydrogen evolution.

4. Conclusion

In this study, the charge/discharge performance of a VRFB was investigated for raw and functionalized (i.e., acid-treated and heat-treated) carbon felt electrodes using symmetric and asymmetric cell configurations. The use of heat-treated electrode in both half-cells was chosen as a baseline case since this combination yielded the best performance. When the positive half-cell in the baseline configuration was changed with raw and acid-treated electrodes, a small deviation was observed in the voltage efficiencies ($\sim 2\%$ difference) for the tested cell configurations, indicating that the surface functionalization has a very small impact on the reaction kinetics in the positive half-cell. However, when the negative half-cell in the baseline configuration was changed with raw and acid-treated electrodes, the voltage efficiencies were observed to change significantly ($\sim 27\%$ deviation), suggesting that the performance of a VRFB is limited by the poor reaction kinetics and high activation losses in the negative half-cell.

To further investigate this observation, a cyclic voltammetry analysis was performed for raw, acid-treated and heat-treated electrodes. The resulting voltammograms indicate that hydrogen evolution occurs very close to the reduction potential for V^{3+} regardless of the functionalization method. This suggests that the poor performance of the negative half-cell reaction is not due to the slow kinetics, but rather arises due to the formation of hydrogen gas bubbles, which block the reaction sites and increase the activation losses. Therefore, one potential approach to increase the performance of a VRFB would be to use electrode materials, which are more kinetically selective to the V^{3+} reduction reaction and yield a peak potential for the reduction reaction which is outside the range of hydrogen evolution.

Acknowledgments

This work was partially supported by the Southern Pennsylvania Ben Franklin Commercialization Institute (Grant #001389-002). K. W. K. greatly acknowledges the support of the National Science Foundation Research Experience for Undergraduates (Grant #235638), and C. R. D. greatly acknowledges the support of the National Science Foundation Integrative Graduate Education and Research Traineeship (Grant #DGE-0654313). The authors would also like to acknowledge Mr. Arvind Kalidindi and Mr. Ahmet Mazacioglu for their assistance and SGL Carbon Group for supplying the electrode material.

References

- [1] M. Skyllas-Kazacos, F. Grossmith, *Journal of The Electrochemical Society* 134 (1987) 2950–2953.
- [2] M. Rychick, M. Skyllas-Kazacos, *Journal of Power Sources* 22 (1988) 59–67.
- [3] D.S. Aaron, Q. Liu, Z. Tang, G.M. Grim, A.B. Papandrew, A. Turhan, T.A. Zawodzinski, M.M. Mench, *Journal of Power Sources* 206 (2012) 450–453.
- [4] L. Yue, W. Li, F. Sun, L. Zhao, L. Xing, *Carbon* 48 (2010) 3079–3090.
- [5] X. Li, K. Huang, S. Liu, N. Tang, L. Chen, *Transactions of Nonferrous Metals Society of China* 17 (2007) 195–199.
- [6] V. Haddadi-ASL, M. Kazacos, M. Skyllas-Kazacos, *Journal of Applied Polymer Science* 57 (1995) 1455–1463.
- [7] Ch. M. Hagg, M. Skyllas-Kazacos, *Journal of Applied Electrochemistry* 32 (2002) 1063–1069.
- [8] H.Q. Zhu, Y.M. Zhang, L. Yue, W.S. Li, G.L. Li, D. Shu, H.Y. Chen, *Journal of Power Sources* 184 (2008) 637–640.
- [9] W. Li, J. Liu, C. Yan, *Electrochimica Acta* 56 (2011) 5290–5294.
- [10] Z. Gonzalez, C. Botas, P. Alvarez, S. Roldan, C. Blanco, R. Santamaria, M. Granda, R. Menendez, *Carbon* 50 (2012) 828–834.
- [11] B. Sun, M. Skyllas-Kazacos, *Electrochimica Acta* 37 (1992) 1253–1260.
- [12] B. Sun, M. Skyllas-Kazacos, *Electrochimica Acta* 37 (1992) 2459–2465.
- [13] S. Zhong, C. Padeste, M. Kazacos, M. Skyllas-Kazacos, *Journal of Power Sources* 45 (1993) 29–41.
- [14] W.H. Wang, X.D. Wang, *Electrochimica Acta* 52 (2007) 6755–6762.
- [15] Y. Shao, X. Wang, M. Engelhard, C. Wang, S. Dai, J. Liu, Z. Yang, Y. Lin, *Journal of Power Sources* 195 (2010) 4375–4379.
- [16] C. Blanc, A. Rufer, *Proceedings of International Conference on Sustainable Energy Technologies, IEEE*, 2008, pp. 696–701.
- [17] A.A. Shah, M.J. Watt-Smith, F.C. Walsh, *Electrochimica Acta* 53 (2008) 8087–8100.
- [18] D. You, H. Zhang, J. Chen, *Electrochimica Acta* 54 (2009) 6827–6836.
- [19] H. Al-Fetlawi, A.A. Shah, F.C. Walsh, *Electrochimica Acta* 55 (2009) 78–89.
- [20] H. Al-Fetlawi, A.A. Shah, F.C. Walsh, *Electrochimica Acta* 55 (2010) 3192–3205.
- [21] A.A. Shah, H. Al-Fetlawi, F.C. Walsh, *Electrochimica Acta* 55 (2010) 1125–1139.
- [22] D. You, H. Zhang, C. Sun, X. Ma, *Journal of Power Sources* 196 (2011) 1578–1585.
- [23] K.W. Knehr, E. Agar, C.R. Dennison, A.R. Kalidindi, E.C. Kumbur, *Journal of The Electrochemical Society* 159 (2012) A1446–A1459.
- [24] K.W. Knehr, E.C. Kumbur, *Electrochemistry Communications* 23 (2012) 76–79.
- [25] S. Kim, J. Yan, B. Schwenzer, J. Zhang, L. Li, J. Liu, Z. Yang, M.A. Hickner, *Electrochemistry Communications* 12 (2010) 1650–1653.
- [26] G. Hwang, H. Ohya, *Journal of Membrane Science* 120 (1996) 55–67.
- [27] K.W. Knehr, E.C. Kumbur, *Electrochemistry Communications* 13 (2011) 342–345.
- [28] A.J. Bard, L.R. Faulkner, *Electrochemical Methods – Fundamentals and Applications*, second ed., Wiley, 2001.